International Journal of Mechanics of Solids

E-ISSN: 2707-8078
P-ISSN: 2707-806X
IJMS 2022; 3(1): 01-19
Received: 05-01-2022
Accepted: 06-02-2022

Akinrinmade Victor Adetayo
Osun State College of Technology, Esa Oke, Osun State, Nigeria

Okeke Onyedika Remigius
Chukwuemeka Odumegwu Ojukwu University, Uli, Anambra state, Nigeria

Afonne Emmanuel
Department of Computer Science & Information Technology, Babcock University, Ilishan-Remo

Corresponding Author:
Akinrinmade Victor Adetayo
Osun State College of Technology, Esa Oke, Osun State, Nigeria

Mathematical formulation F large eddy simulation using hybrid finite difference methods and poisson equations

Akinrinmade Victor Adetayo, Okeke Onyedika Remigius and Afonne Emmanuel

DOI: https://doi.org/10.22271/2707806X.2022.v3.i1a.7

Abstract
This study uses the hybrid finite-difference method (HFDM), which combines the finite-difference and spectral approaches, to describe the Magnetohydrodynamic (MHD) turbulence decay. By using a finite-difference approach in conjunction with a cyclic Penta-diagonal matrix, the numerical algorithm of the hybrid method solves the Navier-Stokes equations and the magnetic field equation with the fourth order's precision in space and second order in time. The spectral approach is used to solve the pressure Poisson equation. The time-dependent turbulence features of this flow were in excellent agreement with the appropriate analytical solution, which is valid for short timeframes, for the classical issue of the 3-D Taylor and Green vortex flow without taking the magnetic field into account. We also show how the effective numerical approach may be utilised to model the decline of magnetohydrodynamic turbulence at various magnetic Reynolds numbers.

Keywords: Spectral approach, hybrid finite difference method, Taylor-Green vortex issue, magnetohydrodynamics, and turbulence decay

1. Introduction
The simulation of cascade processes of turbulent energy transmission, where large- and small-scale vorticity and different turbulence laws intimately interact with each other, is of special interest in studying turbulent flows. Cascade processes determine the internal structure of flows and the method of turbulent dissipation. The study and description of cascade turbulence models received much attention (Kolmogorov, 1941) [25], (Taylor and Green, 1931). Cascade models have mostly been employed to research isotropic turbulence, although they are not without other uses. Building cascade models is crucial for researching the characteristics of magnetohydrodynamic (MHD) turbulence, one of the most complicated turbulent flows.

The first person to bring up the issue of the impact of magnetic fields on turbulent flows was Batchelor (Batchelor, 2021) [2], who offered fundamental equations and an analytical solution for the flow of an electrically conducting fluid. Schumann (1976) [19] conducted the first numerical analysis of the first kind of magnetohydrodynamic turbulence issue with the magnetic number Rem = 1. The hypothesis of (Moffatt, 1967) [26], who investigated a homogeneous isotropic ow affected by an applied external magnetic field, was reflected in the numerical experiment of Schumann. The spectral method is employed in the Modelling described in the works of these scientists, and it serves as the foundation for the presentation of a quantitative description of magnetic damping, the emergence of anisotropy, and the dependence of the results on the presence or absence of a non-linear summand in the Navier-Stokes equation. The limited capabilities of computing devices at the time prevented a complete solution to this issue. A comparable issue was later investigated by (Hossain, 2021) [9] and (Zikanov and Thess, 1998) [24]. Direct numerical Modelling of large-scale structures in a periodic magnetic field was used to get these authors' results. These results showed a change in the statistical turbulence characteristics due to the magnetic field's effect. These scientists' contribution in this field is assessed by demonstrating the significant differences in the behaviour of two- and three-dimensional structures. (Vorobev *et al*., 2005) [22] examined locally isotropic structures using the approach of big eddies and came to a similar conclusion. (Burattini *et al*., 2010) [7], (Knaepen *et al*., 2004) [14], and (Knaepen *et al*., 2004) [14] investigated the process of the magnetic field's influence on developed turbulence. (Knaepen *et al*., 2004) [14].

Demonstrated the possibility of using the quasi-stationary approximation for the solution of the second type of problem and suggested using quasi-linear approximations to solve the problem at $Re_m = 20$. This work aims to investigate weakly induced MHD turbulence flows caused by a homogenous external magnetic field using the current finite-difference and spectral approaches.

The 3-D Taylor and Green vortex flow classic issue is considered for algorithm validation, and it was shown that this flow's simulated time-dependent turbulence characteristics are in great agreement with the corresponding analytical solution valid for short times. In order to characterise the development of three-dimensional turbulence over time (particularly, energy cascade and viscous dissipation), Taylor and Green (1931) developed the classic issue. The resultant flow is now known as the Taylor-Green flow. The fundamental process of turbulent flow inspired their research, the decay of three-dimensional turbulent flow created in a wind tunnel, which was caused by the grinding down of eddies owing to the nonlinearity of the Navier-Stokes equations. They used analysis to calculate the kinetic energy and its rate of dissipation.

Only briefly is Taylor and Green's initial analytical research thorough. Brachet *et al*. (2021) [6] used two approaches to address the Taylor-Green vortex issue to understand better the 3D Taylor-Green vortex flow: numerical solution using the spectral technique and power-series analysis. The resulting average kinetic energy and energy spectra were displayed and contrasted at various flow Reynolds numbers. Three-dimensional Navier-Stokes equations were later numerically integrated with the periodic Taylor-Green starting condition (Brachet *et al*., 2021) [6]. The slope of the energy spectrum was compared with Kolmogorov's 5/3 slope in the inertial subrange in this direct numerical simulation investigation. Additionally, utilising large-eddy simulation and different grid resolutions, the compressible Navier-Stokes equations were also applied to the Taylor-Green vortex issue (DeBonis, 2013) [8], and the temporal evolutions of the kinetic energy and its dissipation rate were compared.

2. Materials and Methods

To estimate the MHD turbulence decay, it is important to numerically model the change in all physical parameters over time at various magnetic Reynolds numbers. This research focuses on the simultaneous investigation of magnetic field self-excitation and conducting fluid motion under the influence of external forces. The goal is to define beginning conditions for the velocity and magnetic fields in the phase space that meet the continuity requirement (Zhakebayev, 2014) [23]. A Fourier transform converts a given starting condition's phase space into physical space. The obtained velocity and magnetic fields are utilised as the filtered MHD equations' beginning conditions. The unstable three-dimensional magnetohydrodynamics equation is also solved to mimic the decay of MHD turbulence. The large eddy simulation method-based numerical Modelling of MHD turbulence degradation dependent on the conductive characteristics of the incompressible fluid is examined. In order to simulate the issue numerically, non-dimensional non-stationary filtered magnetic hydrodynamics equations and the continuity equation are solved in the Cartesian coordinate system.

$$\frac{\partial(u_i)}{\partial t} + \frac{\partial(u_i u_j)}{\partial x_j} = -\frac{\partial(p)}{\partial x_i} + \frac{1}{Re}\frac{\partial}{\partial xj}\left(\frac{\partial(u_i)}{\partial x_j}\right) - \frac{\partial(T_{ij}^H)}{\partial x_j} + A\frac{\partial}{\partial x_j}\left(\overline{H}_i\overline{H}_j\right),$$

$$\frac{\partial\left(\overline{u}_j\right)}{\partial x_j} = 0,$$

$$\frac{\partial\left(\overline{H}_i\right)}{\partial t} + \frac{\partial\left(\overline{u}_j\overline{H}_i\right)}{\partial x_j} - \frac{\partial\left(\overline{H}_j\overline{u}_i\right)}{\partial x_j} = \frac{1}{\mathrm{Re}_m}\frac{\partial}{\partial x_j}\left(\frac{\partial\left(\overline{H}_i\right)}{\partial x_j}\right) - \frac{\partial\left(T_{ij}^H\right)}{\partial x_j},$$

$$\frac{\partial\left(\overline{H}_j\right)}{\partial x_j} = 0,$$

$$T_{ij}^u = \left(\left(\overline{U_iU_j}\right) - \left(\overline{U}_i\overline{U}_j\right)\right) - \left(\left(\overline{H_iH_j}\right) - \left(\overline{H}_i\overline{H}_j\right)\right),$$

$$T_{ij}^H = \left(\left(\overline{U_iH_j}\right) - \left(\overline{U}_i\overline{H}_j\right)\right) - \left(\left(\overline{H_iU_j}\right) - \left(\overline{H}_i\overline{U}_j\right)\right),$$

Where $\bar{u}_i$ (i = 1, 2, 3) are the velocity components, $\bar{H}_1$, $\bar{H}_2$, *and* $\bar{H}_3$ are the magnetic field strength components, $A = H^2/(4\pi\rho V^2) = \Pi/Re^2_m$ is the Alfv'en number, H is the characteristic value of the magnetic field strength, V is the typical velocity, $\Pi = (V_A L/v_m)^2$ is a dimensionless value (on which the value Π depends in the equation for $\bar{H}_i$). If $\Pi << 1$, then $\partial\bar{H}_i/\partial t = 0$. The publication (Ievlev, 1975) discussed the physics of phenomena related to the ability to disregard the summand $\partial\bar{H}_i/\partial t$. $(V_A)^2 = H^2/4\pi\rho$ is the Alfv'en velocity, $\bar{p} = p + \bar{H}^2A/2$ is the full pressure, t is the time, $Re = LV/v$ is the Reynolds number, $Re_m = V L/v_m$ is the magnetic Reynolds number, L is the typical length, v is the kinematic viscosity coefficient, v_m is

the magnetic viscosity coefficient, ρ is the density of electrically conducting incompressible fluid, and τ_{ij}^{u}, τ_{ij}^{H} is the subgrid-scale tensors responsible for small-scale structures to be modelled.

To model a subgrid-scale tensor, a viscosity model is presented as $\tau_{ij}^{u} = -2\nu_T \bar{S}_{ij}$, where

$\nu_T = (C_S\Delta)^2 \left(2\bar{S}_{ij}\bar{S}_{ij}\right)^{\frac{1}{2}}$ is the turbulent viscosity, $\bar{S}_{ij} = (\partial\bar{u}_i/\partial x_j + \partial\bar{u}_j/\partial x_i)/2$ is the deformation velocity tensor value. To model a magnetic subgrid-scale tensor, a viscosity model is used: $\tau_{ij}^{H} = -2\eta_t\bar{J}_{ij}$, where $\eta_t = (D_S\Delta)^2 \left(\bar{J}_{ij}\bar{J}_{ij}\right)^{\frac{1}{2}}$ is the turbulent magnetic diffusion, the coefficients C_S *and* D_S are calculated for each defined time layer, and $\bar{J}_{ij} = (\partial\bar{H}_i/\partial x_j - \partial\bar{H}_j/\partial x_i)/2$ is the magnetic rotation tensor reviewed by (Zhakebayev, 2014) [23].

Periodic boundary conditions are selected at all borders of the reviewed area of the velocity components and the magnetic field strength.

The initial values for each velocity component and strength are defined in the form of a function that depends on the wave numbers in the phase space:

$$u_i(k_i,0) = k_i^{\frac{b-2}{2}} e^{-\frac{b}{4}\left(\frac{k_i}{k_{\max}}\right)^2}; \qquad H_i(k_i,0) = k_i^{\frac{b-2}{2}} e^{-\frac{b}{4}\left(\frac{k_i}{k_{\max}}\right)^2},$$

Where $\bar{u}_i$ is the one-dimensional velocity spectrum, i = 1 refers to the longitudinal spectrum, i = 2, and i = 3 refer to the transverse spectrum, $\bar{H}_i$ is the one-dimensional magnetic field strength spectrum, m is the spectrum power, and k_1, k_2, k_3 are the wave numbers.

For this problem, we selected a variational parameter b and the wave number k_{max}, which determine the type of turbulence. In figure 1, the parameter b varies when k_{max} = 10. For Modelling, homogeneous MHD turbulence can be set parameters k_{max} and b, which correspond to the experimental data [20].

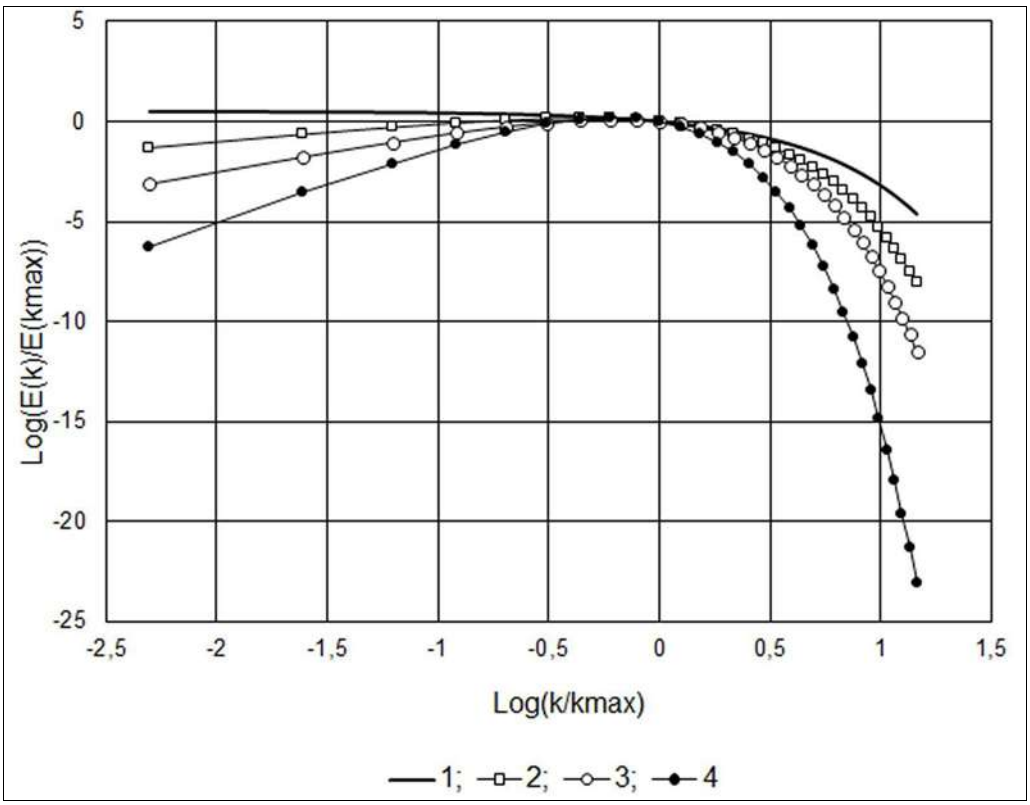

Fig 1: The equation of initial level turbulence, depending on the fixed wave number and the variational parameter b: 1) b = 2; 2) b = 4; 3) b = 6; 4) b = 8.

2.1 Numerical method

To solve the problem of homogeneous incompressible MHD turbulence, a scheme of splitting by physical parameters is used:

1. $(\vec{u}^* - \vec{u}^n)/\Delta t = -(\vec{u}^n\nabla)\vec{u}^* + A(\vec{H}^n\nabla)\vec{H}^n + (1/Re)(\Delta\vec{u}^*) - \nabla\tau^u$,
2. $\Delta p = \nabla\vec{u}^*/\Delta t$,
3. $(\vec{u}^{n+1} - \vec{u}^*)/\Delta t = -\nabla p$.
4. IV. $(\vec{H}^{n+1} - \vec{H}^n)/\Delta t = -rot\left(\vec{u}^{n+1}\times\vec{H}^{n+1}\right) + \left(1/\mathrm{Re}_m\right)\Delta\vec{H}^{n+1} - \nabla T^H$

During the first stage," the Navier-Stokes equation is solved without the pressure consideration. For motion is solved without taking pressure into account. For an approximation of the convective and diffusion terms of the intermediate velocity field, a finite-difference method in combination with a cyclic Penta-diagonal matrix is used (Batista, 2018) [4], (Navon, 1987) [18], which allows for an increase in the order of accuracy in space. The intermediate velocity field is solved using the Adams Bashforth scheme combined with a five-point sweep method. The numerical algorithm for solving incompressible MHD turbulence without considering large eddy simulation is considered (Abdibekova *et al*., 2018). Let's consider the velocity component u_1 in the horizontal direction at the spatial location (i + 1/2,j,k):

$$\frac{\partial u_1}{\partial t}+\frac{\partial(u_1u_1)}{\partial x_1}+\frac{\partial(u_1u_2)}{\partial x_2}+\frac{\partial(u_1u_3)}{\partial x_3}=A\left(\frac{\partial(H_1H_1)}{\partial x_1}+\frac{\partial(H_1H_2)}{\partial x_2}+\frac{\partial(H_1H_3)}{\partial x_3}\right)$$
$$+\frac{1}{\mathrm{Re}}\left(\frac{\partial^2u_1}{\partial x_1^2}+\frac{\partial^2u_1}{\partial x_2^2}+\frac{\partial^2u_1}{\partial x_3^2}\right)-\left(\frac{\partial T_{11}^u}{\partial x_1}+\frac{\partial T_{12}^u}{\partial x_2}+\frac{\partial T_{13}^u}{\partial x_3}\right)$$

When using the explicit Adams-Bachfort scheme for convective terms and the implicit Crank-Nicholson scheme for viscous terms, equation (2) takes the form:
where

$$U^{n+1}_{1_{i+\frac{1}{2},j,k}}-U^{n}_{1_{i+\frac{1}{2},j,k}}=-\frac{3\Delta t}{2}[hx]^n_{i+\frac{1}{2},j,k}+\frac{\Delta t}{2}[hx]^{n-1}_{i+\frac{1}{2},j,k}+\frac{\Delta t}{2}[ax]^n_{i+\frac{1}{2},j,k}+$$
$$\frac{\Delta t}{2}\frac{1}{\mathrm{Re}}\cdot\left[\left(\frac{\partial^2u_1}{\partial x_1^2}\right)^{n+1}_{i+\frac{1}{2},j,k}+\left(\frac{\partial^2u_1}{\partial x_2^2}\right)^{n+1}_{i+\frac{1}{2},j,k}+\left(\frac{\partial^2u_1}{\partial x_3^2}\right)^{n+1}_{i+\frac{1}{2},j,k}\right]+ \quad (3)$$
$$\frac{3\Delta t}{2}[bx]^n_{i+\frac{1}{2},j,k}-\frac{\Delta t}{2}[bx]^{n-1}_{i+\frac{1}{2},j,k}-\frac{3\Delta t}{2}[Tx]^n_{i+\frac{1}{2},j,k}+\frac{\Delta t}{2}[Tx]^{n-1}_{i+\frac{1}{2},j,k}$$

$$[hx]^n_{i+\frac{1}{2},j,k}=\left(\frac{\partial u_1u_1}{\partial x_1}\right)^n_{i+\frac{1}{2},j,k}+\left(\frac{\partial u_1u_2}{\partial x_2}\right)^n_{i+\frac{1}{2},j,k}+\left(\frac{\partial u_1u_3}{\partial x_3}\right)^n_{i+\frac{1}{2},j,k},$$

$$[ax]^n_{i+\frac{1}{2},j,k}=\frac{1}{\mathrm{Re}}\cdot\left[\left(\frac{\partial^2u_1}{\partial x_1^2}\right)^n_{i+\frac{1}{2},j,k}+\left(\frac{\partial^2u_1}{\partial x_2^2}\right)^n_{i+\frac{1}{2},j,k}+\left(\frac{\partial^2u_1}{\partial x_3^2}\right)^n_{i+\frac{1}{2},j,k}\right]$$

$$[bx]^n_{i+\frac{1}{2},j,k}=A\cdot\left[\left(\frac{\partial(H_1H_1)}{\partial x_1}\right)^n_{i+\frac{1}{2},j,k}+\left(\frac{\partial(H_1H_2)}{\partial x_2}\right)^n_{i+\frac{1}{2},j,k}+\left(\frac{\partial(H_1H_3)}{\partial x_3}\right)^n_{i+\frac{1}{2},j,k}\right]$$

$$[Tx]^n_{i+\frac{1}{2},j,k}=\left(\frac{\partial T_{11}^u}{\partial x_1}\right)^n_{i+\frac{1}{2},j,k}+\left(\frac{\partial T_{12}^u}{\partial x_2}\right)^n_{i+\frac{1}{2},j,k}+\left(\frac{\partial T_{13}^u}{\partial x_3}\right)^n_{i+\frac{1}{2},j,k}$$

The discretisation of convective terms looks as [12]:

$$\left(\frac{\partial u_1u_1}{\partial x_1}\right)\Bigg|_{i+\frac{1}{2},j,k}=\frac{-(u_1^2)_{i+2,j,k}+27(u_1^2)_{i+1,j,k}-27(u_1^2)_{i,j,k}+(u_1^2)_{i-1,j,k}}{24\Delta x_1};$$

$$\left(\frac{\partial u_1u_2}{\partial x_2}\right)\Bigg|_{i+\frac{1}{2},j,k}=\frac{(u_1u_2)_{i+\frac{1}{2},j-\frac{3}{2},k}-27(u_1u_2)_{i+\frac{1}{2},j-\frac{1}{2},k}-27(u_1u_2)_{i+\frac{1}{2},j+\frac{1}{2},k}-(u_1u_2)_{i+\frac{1}{2},j+\frac{3}{2},k}}{24\Delta x_2};$$

$$\left(\frac{\partial u_1u_3}{\partial x_3}\right)\Bigg|_{i+\frac{1}{2},j,k}=\frac{(u_1u_3)_{i+\frac{1}{2},j,k-\frac{3}{2}}-27(u_1u_3)_{i+\frac{1}{2},j,k-\frac{1}{2}}+27(u_1u_3)_{i+\frac{1}{2},j,k+\frac{1}{2}}-(u_1u_3)_{i+\frac{1}{2},j,k+\frac{3}{2}}}{24\Delta x_3};$$

The discretisation of diffusion terms looks as:

$$\left(\frac{\partial^2 u_1}{\partial x_1^2}\right)\Bigg|_{i+\frac{1}{2},j,k} = \frac{-(u_1)_{i+\frac{5}{2},j,k} + 16(u_1)_{i+\frac{3}{2},j,k} - 30(u_1)_{i+\frac{1}{2},j,k} + 16(u_1)_{i-\frac{1}{2},j,k} - (u_1)_{i-\frac{3}{2},j,k}}{12\Delta x_1^2};$$

$$\left(\frac{\partial^2 u_1}{\partial x_2^2}\right)\Bigg|_{i+\frac{1}{2},j,k} = \frac{-(u_1)_{i+\frac{1}{2},j+2,k} + 16(u_1)_{i+\frac{1}{2},j+1,k} - 30(u_1)_{i+\frac{1}{2},j,k} + 16(u_1)_{i+\frac{1}{2},j-1,k} - (u_1)_{i+\frac{1}{2},j-2,k}}{12\Delta x_2^2};$$

$$\left(\frac{\partial^2 u_1}{\partial x_3^2}\right)\Bigg|_{i+\frac{1}{2},j,k} = \frac{-(u_1)_{i+\frac{1}{2},j,k+2} + 16(u_1)_{i+\frac{1}{2},j,k+1} - 30(u_1)_{i+\frac{1}{2},j,k} + 16(u_1)_{i+\frac{1}{2},j,k-1} - (u_1)_{i+\frac{1}{2},j,k-2}}{12\Delta x_3^2};$$

Where

$$(u_1u_1)_{i,j,k} = \left(\frac{-u_{1_{i+\frac{3}{2},j,k}} + 9u_{1_{i+\frac{1}{2},j,k}} + 9u_{1_{i-\frac{1}{2},j,k}} - u_{1_{i-\frac{3}{2},j,k}}}{16}\right)^2 (u_1u_2)_{i+\frac{1}{2},j+\frac{1}{2},k} = \left(\frac{-u_{1_{i+\frac{1}{2},j+2,k}} + 9u_{1_{i+\frac{1}{2},j+1,k}} + 9u_{1_{i+\frac{1}{2},j,k}} - u_{1_{i+\frac{1}{2},j-1,k}}}{16}\right).$$

$$\cdot\left(\frac{-u_{2_{i+2,j+\frac{1}{2},k}} + 9u_{2_{i+1,j+\frac{1}{2},k}} + 9u_{2_{i,j+\frac{1}{2},k}} - u_{2_{i-1,j+\frac{1}{2},k}}}{16}\right)$$

$$(u_1u_3)_{i+\frac{1}{2},j,k+\frac{1}{2}} = \left(\frac{-u_{1_{i+\frac{1}{2},j,k+2}} + 9u_{1_{i+\frac{1}{2},j,k+1}} + 9u_{1_{i+\frac{1}{2},j,k}} - u_{1_{i+\frac{1}{2},j,k-1}}}{16}\right).;$$

$$\cdot\left(\frac{-u_{3_{i+2,j,k+\frac{1}{2}}} + 9u_{3_{i+1,j,k+\frac{1}{2}}} + 9u_{3_{i,j,k+\frac{1}{2}}} - u_{3_{i-1,j,k+\frac{1}{2}}}}{16}\right);$$

The discretisation of magnetic field terms looks as: $\frac{H^2}{} \quad \frac{H^2}{} +$

$$\left(\frac{\partial(H_1H_1)}{\partial x_1}\right)\Bigg|_{i+\frac{1}{2},j,k} = \frac{-(1)i+2,j,k+27(1)i+1,j,k}{24\Delta x_1}$$

$$\frac{27(H_1^2)_{i,j,k} + (H_1^2)i-1,j,k}{24\Delta x_1}$$

$$\left(\frac{\partial(H_1H_2)}{\partial x_1}\right)\Bigg|_{i+\frac{1}{2},j,k} = \frac{(H_1H_2)_{i+\frac{1}{2},j-\frac{3}{2},k} - 27(H_1H_2)_{i+\frac{1}{2},j-\frac{1}{2},k}}{24\Delta x_2} +$$

$$+\frac{27(H_1H_2)_{i+\frac{1}{2},j+\frac{1}{2},k}-(H_1H_2)_{i+\frac{1}{2},j+\frac{3}{2},k}}{24\Delta x_2};$$

$$\left(\frac{\partial(H_1H_3)}{\partial x_3}\right)\Big|_{i+\frac{1}{2},j,k}=\frac{(H_1H_3)_{i+\frac{1}{2},j,k-\frac{3}{2}}-27(H_1H_3)_{i+\frac{1}{2},j,k-\frac{1}{2}}}{24\Delta x_3}+$$

$$+\frac{27(H_1H_3)_{i+\frac{1}{2},j,k+\frac{1}{2}}-(H_1H_3)_{i+\frac{1}{2},j,k+\frac{3}{2}}}{24\Delta x_3};$$

The viscosity model and the subgrid-scale tensor are, respectively,

$$T_{11}^u=-2\nu_T.S_{11} \qquad S_{11}=\frac{1}{2}\left(\frac{\partial u_1}{\partial x_1}+\frac{\partial u_1}{\partial x_1}\right)=0$$

$$T_{12}^u=-2\nu_T.S_{12} \qquad S_{12}=\frac{1}{2}\left(\frac{\partial u_1}{\partial x_2}+\frac{\partial u_2}{\partial x_1}\right)$$

$$T_{13}^u=-2\nu_T.S_{13} \qquad S_{13}=\frac{1}{2}\left(\frac{\partial u_1}{\partial x_3}+\frac{\partial u_3}{\partial x_1}\right)$$

The discretisation of the strength tensor terms looks as:

$$\left(\frac{\partial(-T_{11}^u)}{\partial x_1}\right)\Big|_{i+\frac{1}{2},j,k}=\frac{\partial}{\partial x_1}(2\nu_T.S_{11})=\frac{2}{\Delta x_1}\left[\begin{array}{l}(\nu_T)_{i+\frac{1}{2},j,k}.\left[\frac{(u_1)_{i+1,j,k}-(u_1)_{i,j,k}}{\Delta x_1}\right]+\\+(\nu_T)_{i-\frac{1}{2},j,k}.\left[\frac{(u_1)_{i,j,k}-(u_1)_{i-1,j,k}}{\Delta x_1}\right]\end{array}\right]=0$$

$$\left(\frac{\partial(-T_{12}^u)}{\partial x_2}\right)\Big|_{i+\frac{1}{2},j,k}=\frac{\partial}{\partial x_2}(2\nu_T.S_{12})=\frac{2}{2.\Delta x_2}\left[\begin{array}{l}(\nu_T)_{i,j+\frac{1}{2},k}.\left[\frac{(u_1)_{i,j+1,k}-(u_1)_{i,j,k}}{\Delta x_2}-\frac{(u_2)_{i+1,j,k}-(u_2)_{i,j,k}}{\Delta x_1}\right]+\\+(\nu_T)_{i,j-\frac{1}{2},k}.\left[\frac{(u_1)_{i,j,k}-(u_1)_{i,j-1,k}}{\Delta x_2}-\frac{(u_2)_{i,j,k}-(u_2)_{i-1,j,k}}{\Delta x_1}\right]\end{array}\right]$$

$$\left(\frac{\partial(-T_{13}^u)}{\partial x_3}\right)\Big|_{i+\frac{1}{2},j,k}=\frac{\partial}{\partial x_3}(2\nu_T.S_{13})=\frac{2}{2.\Delta x_3}\left[\begin{array}{l}(\nu_T)_{i,j,k+\frac{1}{2}}.\left[\frac{(u_1)_{i,j,k+1}-(u_1)_{i,j,k}}{\Delta x_3}-\frac{(u_3)_{i+1,j,k}-(u_3)_{i,j,k}}{\Delta x_1}\right]+\\+(\nu_T)_{i,j,k-\frac{1}{2}}.\left[\frac{(u_1)_{i,j,k}-(u_1)_{i,j,k-1}}{\Delta x_3}-\frac{(u_3)_{i,j,k}-(u_3)_{i-1,j,k}}{\Delta x_1}\right],\end{array}\right]$$

Then the left-hand side of equation (3) is denoted by $q_{i+\frac{1}{2}jk}$

$$q_{i+\frac{1}{2}jk}\equiv U_{1\,i+\frac{1}{2}j,k}^{n+1}-U_{1\,i+\frac{1}{2}j,k}^{n} \tag{4}$$

We find $U_{1\,i+\frac{1}{2}jk}^{n+1}$ from equation (4)

$$U_{1\,i+\frac{1}{2}j,k}^{n+1}=q_{i+\frac{1}{2}jk}+U_{1\,i+\frac{1}{2}j,k}^{n}.$$

Replacing all $U_{1\,i+\frac{1}{2}j,k}^{n+1}$ – the equations (3), we obtain

$$q_{i+\frac{1}{2}jk} - \frac{\Delta t}{2}\cdot\frac{1}{\mathrm{Re}}\cdot\left(\frac{\partial^2 q}{\partial x_1^2}\right)_{i+\frac{1}{2}j,k} - \frac{\Delta t}{2}\cdot\frac{1}{\mathrm{Re}}\cdot\left(\frac{\partial^2 q}{\partial x_2^2}\right)_{i+\frac{1}{2}j,k} - \frac{\Delta t}{2}\cdot\frac{1}{\mathrm{Re}}\cdot\left(\frac{\partial^2 q}{\partial x_3^2}\right)_{i+\frac{1}{2}j,k} =$$

$$-3\frac{\Delta t}{2}[hx]_{i+\frac{1}{2},j,k}^{n} + \frac{\Delta t}{2}[hx]_{i+\frac{1}{2},j,k}^{n-1} + \Delta t[ax]_{i+\frac{1}{2},j,k}^{n} + \frac{3\Delta t}{2}[bx]_{i+\frac{1}{2},j,k}^{n} - \frac{\Delta t}{2}[bx]_{i+\frac{1}{2},j,k}^{n-1} -$$

$$\frac{3\Delta t}{2}[Tx]_{i+\frac{1}{2},j,k}^{n} + \frac{\Delta t}{2}[Tx]_{i+\frac{1}{2},j,k}^{n-1},$$

We can re-write equation (5) as

$$\left[1-\frac{\Delta t}{2}\cdot\frac{1}{\mathrm{Re}}\cdot\frac{\partial^2}{\partial x_1^2} - \frac{\Delta t}{2}\cdot\frac{1}{\mathrm{Re}}\cdot\frac{\partial^2}{\partial x_2^2} - \frac{\Delta t}{2}\cdot\frac{1}{\mathrm{Re}}\cdot\frac{\partial^2}{\partial x_3^2}\right]q_{i+\frac{1}{2}jk} = d_{i+\frac{1}{2},j,k}, \tag{6}$$

Where

$$d_{i+\frac{1}{2}jk} = -3\frac{\Delta t}{2}[hx]_{i+\frac{1}{2},j,k}^{n} + \frac{\Delta t}{2}[hx]_{i+\frac{1}{2},j,k}^{n-1} + \Delta t[ax]_{i+\frac{1}{2},j,k}^{n} + \frac{3\Delta t}{2}[bx]_{i+\frac{1}{2},j,k}^{n} - \frac{\Delta t}{2}[bx]_{i+\frac{1}{2},j,k}^{n-1} -$$

$$\frac{3\Delta t}{2}[Tx]_{i+\frac{1}{2},j,k}^{n} + \frac{\Delta t}{2}[Tx]_{i+\frac{1}{2},j,k}^{n-1}$$

Assuming that equation (6) has the second-order accuracy in time, we may solve the following equation instead:

$$\left[1-\frac{\Delta t}{2}\cdot\frac{1}{\mathrm{Re}}\frac{\partial^2}{\partial x_1^2}\right]\left[1-\frac{\Delta t}{2}\frac{1}{\mathrm{Re}}\cdot\frac{\partial^2}{\partial x_2^2}\right]\left[1-\frac{\Delta t}{2}\cdot\frac{1}{\mathrm{Re}}\frac{\partial^2}{\partial x_3^2}\right]q^{*}_{i+\frac{1}{2}jk} = d_{i+\frac{1}{2},j,k} \tag{7}$$

We can show that equation (7) is an $O(\Delta t^4)$ approximation to equation (6) (Kim and Moin, 1985). Equation (7) is a factorisation approximation to equation (6), which allows each spatial direction to be treated sequentially. If we denote the solution to equation (7) $q^{*}_{i+\frac{1}{2}jk}$ by expanding equation (7), subtracting equation (6) from it, and noting that

$q_{i+\frac{1}{2}jk} \square o\left(\Delta t^2\right)$, we obtain $\left(q^{*}_{i+\frac{1}{2}jk} - q_{i+\frac{1}{2}jk}\right) \square o\left(\Delta t^4\right)$

Therefore, equation (7) is an order O (Δt^4) approximation to equation (6) rather than an order O (Δt^3) approximation as stated in (Kim and Moin, 1985) without proof. Since the difference between $q^{*}_{i+\frac{1}{2}jk}$ and $q_{i+\frac{1}{2}jk}$ is of higher order, we shall return to the same notation and just use $q_{i+\frac{1}{2}jk}$ To determine $q_{i+\frac{1}{2}jk}$, equation (7) is solved in 3 stages in sequence as follows:

$$\left[1-\frac{\Delta t}{2}\cdot\frac{1}{\mathrm{Re}}\cdot\frac{\partial^2}{\partial x_1^2}\right]A_{i+\frac{1}{2},j,k} = d_{i+\frac{1}{2},j,k}; \tag{8}$$

$$\left[1-\frac{\Delta t}{2}\cdot\frac{1}{\mathrm{Re}}\cdot\frac{\partial^2}{\partial x_2^2}\right]B_{i+\frac{1}{2},j,k} = A_{i+\frac{1}{2},j,k}; \tag{9}$$

$$\left[1-\frac{\Delta t}{2}\cdot\frac{1}{\mathrm{Re}}\cdot\frac{\partial^2}{\partial x_3^2}\right]q_{i+\frac{1}{2},j,k} = B_{i+\frac{1}{2}jk}. \tag{10}$$

In the first stage, $A_{i+\frac{1}{2},j,k}$ it is sought in the coordinate direction x_1

$$\frac{{}_{S_1}A_{i+\frac{5}{2},j,k} - 16_{S_1}A_{i+\frac{3}{2},j,k} + (1+30_{S_1})A_{i+\frac{1}{2},j,k} -}{12\Delta x_1^2} +$$

$$\left[1 - \frac{\Delta t}{2}.\frac{1}{\mathrm{Re}}.\frac{\partial^2}{\partial x_1^2}\right]A_{i+\frac{1}{2},j,k} = d_{i+\frac{1}{2},j,k}, + \frac{16A_{i+\frac{1}{2},j,k} - A_{i-\frac{3}{2},j,k}}{12\Delta x_1^2} = d_{i+\frac{1}{2},j,k}'$$

$$A_{i+\frac{1}{2},j,k} - \frac{\Delta t}{2}.\frac{1}{\mathrm{Re}}.\left(\frac{\partial^2 A}{\partial x_1^2}\right)_{i+\frac{1}{2},j,k} = d_{i+\frac{1}{2},j,k},$$

$${}_{S_1}A_{i+\frac{5}{2},j,k} - 16_{S_1}A_{i+\frac{3}{2},j,k} + (1+30_{S_1})A_{i+\frac{1}{2},j,k} - 16_{S_1}A_{i-\frac{1}{2},j,k} + {}_{S_1}A_{i-\frac{3}{2},j,k} = d_{i+\frac{1}{2},j,k} \quad (12)$$

where ${}_{S_1} = \frac{\Delta t}{24.\mathrm{Re}.\Delta x_1^2}$.

This equation (12) is solved by the cyclic Penta-diagonal matrix, which yields.

$$A_{i+\frac{1}{2},j,k}$$

The same procedure is repeated for the x_2 directions in the second stage. Namely, $B_{i+\frac{1}{2},jk}$ it is obtained by solving equation (9), with the solution from the first stage as the coefficient on the right hand and the coefficient s_1 in the Penta-diagonal matrix replaced by

$${}_{S_2} = \frac{\Delta t}{24.\mathrm{Re}.\Delta x_2^2}$$

Finally, the third stage $q_{i+\frac{1}{2},jk}$ is solved through the similar Penta-diagonal the system is shown in equation (10).

Once we have determined the value $q_{i+\frac{1}{2},j,k}$, we find $U_{1_{i+\frac{1}{2},j,k}}^{n+1}$

$$U_{1_{i+\frac{1}{2},j,k}}^{n+1} = q_{i+\frac{1}{2},j,k} + U_{1_{i+\frac{1}{2},j,k}}^{n}.$$

The velocity components $U_{2_{i,j+\frac{1}{2},k}}^{n+1}$ $U_{3_{i,j,k+\frac{1}{2},k}}^{n+1}$ are solved similarly.

2.3 Algorithm for solving the Poisson equation

The pressure Poisson equation is solved in the subsequent phase, ensuring that the continuity equation is satisfied. A Fourier transform converts the Poisson equation from physical space to spectral space. The continuity equation is not satisfied by the resultant intermediate velocity field. The term corresponding to the pressure gradient is added to the intermediate field to produce the final velocity field:

$$u_1^{n+1} = u_1^{n+1} - \Delta t \frac{\partial p}{\partial x_1}$$

$$u_2^{n+1} = u_2^{n+1} - \Delta t \frac{\partial p}{\partial x_2} \; ; \; u_3^{n+1} = u_3^{n+1} - \Delta t \frac{\partial^2 p}{\partial x_3}$$

Substituting the continuity equation, we obtain the Poisson equation for the pressure field:

$$\frac{\partial^2 p}{\partial x_1^2} + \frac{\partial^2 p}{\partial x_2^2} + \frac{\partial^2 p}{\partial x_3^2} = \Delta t \left(\frac{\partial u_1^{n+1}}{\partial x_1} + \frac{\partial u_2^{n+1}}{\partial x_2} + \frac{\partial u_3^{n+1}}{\partial x_3} \right) = F_{i,j,k},$$

Where $F_{i,j,k}$ denotes the known right-hand side of the Poisson equation, each term is approximated by an order $O(\Delta x^4)$ finite-difference approximation. For example, the first term in $F_{i,j,k}$ is approximated as

$$\Delta t \frac{\partial u_1^{n+1}}{\partial x_1}\Bigg|_{i+\frac{1}{2},j,k} = \Delta t \frac{u^{n+1}_{1i-\frac{3}{2},j,k} - 8u^{n+1}_{1i-\frac{1}{2},j,k} + 8u^{n+1}_{1i+\frac{3}{2},j,k} - u^{n+1}_{1i-\frac{5}{2},j,k}}{12\Delta x_1}$$

To be consistent with the spatial accuracy in the first step, the left-hand side of the above Poisson equation is discretised using the 5-point scheme of $O(\Delta x^4)$ accuracy, as follows:

$$\left[\frac{-P_{i+2,j,k} + 16P_{i+1,j,k} - 30P_{i,j,k} + 16P_{i-1,j,k} - P_{i-2,j,k}}{12\Delta x_1^2} \right] +$$

$$\left[\frac{-P_{i,j+2,k} + 16P_{i,j+1,k} - 30P_{i,j,k} + 16P_{i,j-1,k} - P_{i,j-2,k}}{12\Delta x_2^2} \right] +$$

$$\left[\frac{-P_{i,j,k+2} + 16P_{i,j,k+1} - 30P_{i,j,k} + 16P_{i,j,k-1} - P_{i,j,k-2}}{12\Delta x_3^2} \right] = F_{i,j,k} \quad (13)$$

Now we apply the three-dimensional Fourier transform.

$$P_{i,j,k} = \frac{1}{N} \sum^{N_1-1} \sum^{N_2-1} \sum^{N_3-1} V_1^{im} V_2^{jn} V_3^{sk} . p_{m,n,s} \; ;$$

$$F_{i,j,k} = \frac{1}{N} \sum_{m=0}^{N_1-1} \sum_{n=0}^{N_2-1} \sum_{s=0}^{N_3-1} V_1^{im} V_2^{jn} V_3^{sk} . f_{m,n,s} \quad (14)$$

The inverse transforms are:

$$f_{m,n,s} = \frac{1}{N} \sum_{i=0}^{N_1-1} \sum_{j=0}^{N_2-1} \sum_{k=0}^{N_3-1} V_1^{-im} V_2^{-jn} V_3^{-sk} . F_{i,j,k}$$

$$p_{m,n,s} = \frac{1}{N} \sum^{N_1-1} \sum^{N_2-1} \sum^{N_3-1} V_1^{-im} V_2^{-jn} V_3^{-sk} . P_{i,j,k} \; ; \quad (15)$$

.

Where $N = N_1 . N_2 . N_3, V_1 = e^{I\left(\frac{2\pi}{N_1}\right)}, V_2 = e^{I\left(\frac{2\pi}{N_2}\right)}$ ——, and $V_3 = e^{I\left(\frac{2\pi}{N3}\right)}$.

Substituting equation (15) into equation (14), we obtain the solution for the pressure field quickly in the spectral space as

$$pm,n,s=\frac{12\,fm,n,s}{Q_1+Q_2+Q_3} \tag{16}$$

Where

$$\left[-2\cos\left(\frac{4\pi m}{N_1}\right)+32\cos\left(\frac{2\pi m}{N_1}\right)-30\right]$$
$$\left[-2\cos\left(\frac{4\pi n}{N_2}\right)+32\cos\left(\frac{2\pi n}{N_2}\right)-30\right]$$
$$\left[-2\cos\left(\frac{4\pi s}{N_3}\right)+32\cos\left(\frac{2\pi s}{N_3}\right)-30\right]$$

The pressure Pi, j, and k in the physical space are then calculated using an inverse Fourier transform. The final velocity field is then calculated using the acquired pressure field in the third stage. When the final velocity field is computed, the third step assumes that the transfer is exclusively accomplished through the pressure gradient. ($\vec{u}^{n+1}-\vec{u}^{*})/\Delta t=-\nabla p$).

2.4 An algorithm for resolving the magnetic field strength equation

Reviewing equation (1) for the first component of the horizontal magnetic field intensity at the geographical location (i + 1/2, j, k): (17)

$$\frac{\partial H_1}{\partial t}+\frac{\partial}{\partial x_2}\left(u_2H_1-H_2u_1\right)+\frac{\partial}{\partial x_3}\left(u_3H_1-H_3u_1\right)-$$
$$-\frac{1}{\mathrm{Re}_m}\left[\frac{\partial^2H_1}{\partial x_1^2}+\frac{\partial^2H_1}{\partial x_2^2}\frac{\partial^2H_1}{\partial x_3^2}\right]=-\left(\frac{\partial_{T_{11}^H}}{\partial x_1}+\frac{\partial_{T_{12}^H}}{\partial x_2}+\frac{\partial_{T_{13}^H}}{\partial x_3}\right).$$

Equation (17) results from finding the magnetic field strength using the explicit Adams-Bachfort method for magnetic convective terms and the implicit Crank-Nicholson strategy for viscous terms.

$$H_{1\,i+\frac{1}{2},j,k}^{n+1}-H_{1\,i+\frac{1}{2},j,k}^{n}=-\frac{3\Delta t}{2}[Hx]_{i+\frac{1}{2},j,k}^{n}+\frac{\Delta t}{2}[Hx]_{i+\frac{1}{2},j,k}^{n-1}+\frac{\Delta t}{2}[aHx]_{i+\frac{1}{2},j,k}^{n}+$$
$$+\frac{\Delta t}{2}\frac{1}{\mathrm{Re}}.\left[\left(\frac{\partial^2H_1}{\partial x_1^2}\right)_{i+\frac{1}{2},j,k}^{n+1}+\left(\frac{\partial^2H_1}{\partial x_2^2}\right)_{i+\frac{1}{2},j,k}^{n+1}+\left(\frac{\partial^2H_1}{\partial x_3^2}\right)_{i+\frac{1}{2},j,k}^{n+1}\right]- \tag{18}$$
$$-\frac{3\Delta t}{2}[{}_T Hx]_{i+\frac{1}{2},j,k}^{n}+\frac{\Delta t}{2}[{}_T Hx]_{i+\frac{1}{2},j,k}^{n-1}$$

Where

$$[Hx]_{i+\frac{1}{2},j,k}^{n}=\left[\frac{\partial}{\partial x_2}(u_2H_1-H_2u_1\right]_{i+\frac{1}{2},j,k}^{n}+\left[\frac{\partial}{\partial x_3}(u_3H_1-H_3u_1\right]_{i+\frac{1}{2},j,k}^{n}$$

$$[aHx]_{i+\frac{1}{2},j,k}^{n}=\frac{1}{\mathrm{Re}_m}.\left[\left(\frac{\partial^2H_1}{\partial x_1^2}\right)_{i+\frac{1}{2},j,k}^{n}+\left(\frac{\partial^2H_1}{\partial x_2^2}\right)_{i+\frac{1}{2},j,k}^{n}+\left(\frac{\partial^2H_1}{\partial x_3^2}\right)_{i+\frac{1}{2},j,k}^{n}\right]$$

$$[{}_T Hx]_{i+\frac{1}{2}jk}^{n}=\left(\frac{\partial_{T_{11}^u}}{\partial x_1}\right)_{i+\frac{1}{2},j,k}^{n}+\left(\frac{\partial_{T_{12}^u}}{\partial x_2}\right)_{i+\frac{1}{2},j,k}^{n}+\left(\frac{\partial_{T_{13}^u}}{\partial x_3}\right)_{i+\frac{1}{2},j,k}^{n}$$

The discretisation of magnetic convective terms looks as:

$$\left(\frac{\partial u_2 u_1}{\partial x_2}\right)\Big|_{i+\frac{1}{2},j,k} = \frac{(u_2H_1)_{i+\frac{1}{2},j-\frac{3}{2},k} - 27(u_2H_1)_{i+\frac{1}{2},j-\frac{1}{2},k} + 27(u_2H_1)_{i+\frac{1}{2},j+\frac{1}{2},k} - (u_2H_1)_{i+\frac{1}{2},j+\frac{3}{2},k}}{24\Delta x_2};$$

$$\left(\frac{\partial H_2 u_1}{\partial x_2}\right)\Big|_{i+\frac{1}{2},j,k} = \frac{(H_2u_1)_{i+\frac{1}{2},j-\frac{3}{2},k} - 27(H_2u_1)_{i+\frac{1}{2},j-\frac{1}{2},k} + 27(H_2u_1)_{i+\frac{1}{2},j+\frac{1}{2},k} - (H_2u_1)_{i+\frac{1}{2},j+\frac{3}{2},k}}{24\Delta x_2};$$

$$\left(\frac{\partial H_3 u_1}{\partial x_3}\right)\Big|_{i+\frac{1}{2},j,k} = \frac{(H_3u_1)_{i+\frac{1}{2},j,k-\frac{3}{2}} - 27(H_3u_1)_{i+\frac{1}{2},j,k-\frac{1}{2}} + 27(H_3u_1)_{i+\frac{1}{2},j,k+\frac{1}{2}} - (H_3u_1)_{i+\frac{1}{2},j,k+\frac{3}{2}}}{24\Delta x_3};$$

$$\left(\frac{\partial u_3 H_1}{\partial x_3}\right)\Big|_{i+\frac{1}{2},j,k} = \frac{(u_3H_1)_{i+\frac{1}{2},j,k-\frac{3}{2}} - 27(u_3H_1)_{i+\frac{1}{2},j,k-\frac{1}{2}} + 27(u_3H_1)_{i+\frac{1}{2},j,k+\frac{1}{2}} - (u_3H_1)_{i+\frac{1}{2},j,k+\frac{3}{2}}}{24\Delta x_3};$$

The discretisation of magnetic diffusion terms looks as:

$$\left(\frac{\partial^2 H_1}{\partial x_1^2}\right)\Big|_{i+\frac{1}{2},j,k} = \frac{-(H_1)_{i+\frac{5}{2},j,k} + 16(H_1)_{i+\frac{3}{2},j,k} - 30(H_1)_{i+\frac{1}{2},j,k}}{12\Delta x_1^2} +$$

$$+ \frac{16(H_1)_{i-\frac{1}{2},j,k} - (H_1)_{i-\frac{3}{2},j,k}}{12\Delta x_1^2}$$

$$\left(\frac{\partial^2 H_1}{\partial x_2^2}\right)\Big|_{i+\frac{1}{2},j,k} = \frac{-(H_1)_{i+\frac{1}{2},j+2,k} + 16(H_1)_{i+\frac{1}{2},j+1,k} - 30(H_1)_{i+\frac{1}{2},j,k}}{12\Delta x_2^2} +$$

$$H \qquad\qquad H$$

$$+ \frac{16(\quad 1)_{i+\frac{1}{2},j-1,k} - (\quad 1)_{i+\frac{1}{2},j-2,k}}{12\Delta x_2^2};$$

$$\left(\frac{\partial^2 H_1}{\partial x_3^2}\right)\Big|_{i+\frac{1}{2},j,k} = \frac{-(H_1)_{i+\frac{1}{2},j,k+2} + 16(H_1)_{i+\frac{1}{2},j,k+1} - 30(H_1)_{i+\frac{1}{2},j,k}}{12\Delta x_3^2} +$$

$$+ \frac{16(H_1)_{i+\frac{1}{2},j,k-1} - (H_1)_{i+\frac{1}{2},j,k-2}}{12\Delta x_3^2},$$

Where

$$(u_2H_1)_{i+\frac{1}{2},j+\frac{1}{2},k} = \left(\frac{-u2i+2, j+\frac{1}{2}'k + 9u2i+1, j+\frac{1}{2}'k + 9u2i+1, j+\frac{1}{2}'k - u2i-1, j+\frac{1}{2}'k}{16}\right)$$

$$\left(\frac{-H_{1_{i+\frac{1}{2},j+2,k}} + 9H_{1_{i+\frac{1}{2},j+1,k}} + 9H_{1_{i+\frac{1}{2},j,k}} - H_{1_{i+\frac{1}{2},j-1,k}}}{16}\right);$$

$$(H_2u_1)_{i+\frac{1}{2},j+\frac{1}{2},k} = \left(\frac{-H_{2_{i+2,j+\frac{1}{2},k}} + 9H_{2_{i+1,j+\frac{1}{2},k}} + 9H_{2_{i,j+\frac{1}{2},k}} - H_{2_{i+1,j+\frac{1}{2},k}}}{16} \right.$$

$$\left. \frac{-u1i+\frac{1}{2},j+2,k + 9u1i+\frac{1}{2},j+1,k + 9u1i+\frac{1}{2},j,k - u1i+\frac{1}{2},j-1,k}{16} \right);$$

$$(u_3H_1)_{i+\frac{1}{2},j,k+\frac{1}{2}} = \left(\frac{-u3i+2,\ j,k+\frac{1}{2} + 9u3i+1,\ j,k+\frac{1}{2} + 9u3i,\ j,k+\frac{1}{2} - u3i-1,\ j,k+\frac{1}{2}}{16} \right.$$

$$\left. \frac{-H_{1_{i+\frac{1}{2},j,k+2}} + 9H_{1_{i+\frac{1}{2},j,k+1}} + 9H_{1_{i+\frac{1}{2},j,k}} - H_{1_{i+\frac{1}{2},j,k-1}}}{16} \right)$$

The viscosity model and the magnetic rotation tensor are, respectively,

$$T_{11}^H = -2\eta_t.J_{11}, \qquad J_{11} = \frac{1}{2}\left(\frac{\partial H_1}{\partial x_1} - \frac{\partial H_1}{\partial x_1} \right) = 0,$$

$$T_{12}^H = -2\eta_t.J_{12}, \qquad J_{12} = \frac{1}{2}\left(\frac{\partial H_1}{\partial x_2} - \frac{\partial H_2}{\partial x_1} \right),$$

$$T_{13}^H = -2\eta_t.J_{13}, \qquad J_{13} = \frac{1}{2}\left(\frac{\partial H_1}{\partial x_3} - \frac{\partial H_3}{\partial x_1} \right),$$

The discretisation of the magnetic rotation tensor terms looks as:

$$\frac{\partial}{\partial x_1}(-T_{11}^H) = 0,$$

$$= \frac{2}{2.\Delta x_2}\left[(\eta_t)_{i,j+\frac{1}{2},k} \cdot \left[\frac{(H_1)_{i,j+1,k} - (H_1)_{i,j,k}}{\Delta x_2} - \frac{(H_{2)_{i+1,j,k}} - (H_2)_{i,j,k}}{\Delta x_1} \right] - \right.$$
$$\left. -(\eta_t)_{i,j-\frac{1}{2},k} \cdot \left[\frac{(H_1)_{i,j,k} - (H_1)_{i,j-1,k}}{\Delta x_2} - \frac{(H_2)_{i,j,k} - (H_2)_{i-1,j,k}}{\Delta x_1} \right] \right]$$

$$\frac{\partial}{\partial x_3}(-T_{13}^H) = \frac{\partial}{\partial x_3}(2\eta_t.J_{13}) =$$

$$= \frac{2}{2.\Delta x_3}\left[(\eta_t)_{i,j,k+\frac{1}{2}} \cdot \left[\frac{(H_1)_{i,j,k+1} - (H_1)_{i,j,k}}{\Delta x_3} - \frac{(H_{3)_{i+1,j,k}} - (H_3)_{i,j,k}}{\Delta x_1} \right] - \right.$$
$$\left. -(\eta_t)_{i,j,k-\frac{1}{2}} \cdot \left[\frac{(H_1)_{i,j,k} - (H_1)_{i,j,k-1}}{\Delta x_3} - \frac{(H_3)_{i,j,k} - (H_3)_{i-1,j,k}}{\Delta x_1} \right] \right]$$

The equation is solved by the similar Penta-diagonal system shown in section II and is found to be

$$(H_1)_{i,j,k.}^{n+\frac{1}{3}}$$

$$(H_1)_{i,j,k.}^{n+\frac{2}{3}}, (H_1)_{i,j,k}^{n+1}$$

Components of the magnetic field strength are defined similarly.
Thus, all the components of the magnetic field strength are determined this way.

2.5 Definition of homogeneous MHD turbulence characteristics

It is important to average several volumetric values to determine turbulence properties in the physical space. The numbers that have been averaged will be utilised to identify the turbulent properties. The method described in articles by (Monin and Yaglom, 1975) and for computing the turbulence properties is similar to that described in (Batchelor 2019) [3]. The following formula is used to determine the value averaged throughout the full computed area.

$$\{u_i\} = \frac{1}{N_1 N_2 N_3} \sum_{n=1}^{N_1} \sum_{m=1}^{N_2} \sum_{q=1}^{N_3} \left(\bar{u}_i\right)_{n,m,q}$$

$$\{H_i\} = \frac{1}{N_1 N_2 N_3} \sum_{n=1}^{N_1} \sum_{m=1}^{N_2} \sum_{q=1}^{N_3} \left(\overline{H}_i\right)_{n,m,q}$$

$$\left\{u_1^2\right\} = \left\{u_1\left(x,y,z,t\right).u_1\left(x,y,z,t\right)\right\},$$

$$\left\{u_2^2\right\} = \left\{u_2\left(x,y,z,t\right).u_2\left(x,y,z,t\right)\right\},$$

$$\left\{u_3^2\right\} = \left\{u_3\left(x,y,z,t\right).u_3\left(x,y,z,t\right)\right\}.$$

The following ratio determines the microscale length:

$$\lambda_f = \left\{\frac{2}{-f''(0)}\right\}^{\frac{1}{2}}, \lambda_g = \left\{\frac{2}{-g''(0)}\right\}^{\frac{1}{2}}$$

The integral scale is expressed as

$$\Lambda_f(t) = \int_0^{L/2} f(r,t)dr, \qquad \Lambda_g(t) = \int_0^{L/2} g(r,t)dr.$$

The following formula calculates the dissipation rate:

$$\in = < 2\nu S_{ij} S_{ij} > = 2\nu\left[\left\{\left(\frac{\partial u_1}{\partial x_1}\right)^2\right\} + \left\{\left(\frac{\partial u_2}{\partial x_2}\right)^2\right\} + \left\{\left(\frac{\partial u_3}{\partial x_3}\right)^2\right\}\right] +$$

$$2\nu\left[\frac{1}{2}\left\{\left(\frac{\partial u_1}{\partial x_2} + \frac{\partial u_2}{\partial x_1}\right)\right\} + \frac{1}{2}\left\{\left(\frac{\partial u_1}{\partial x_3} + \frac{\partial u_3}{\partial x_1}\right)\right\} + \frac{1}{2}\left\{\left(\frac{\partial u_2}{\partial x_3} + \frac{\partial u_3}{\partial x_2}\right)\right\}\right]$$

The turbulent kinematic energy is found in the following way: The turbulent kinetic and magnetic energy are, respectively,

$$E_{ku} = \frac{1}{2}\left(\{u_1\}^2 + \{u_2\}^2 + \{u_3\}^2\right) = \frac{3}{2}\left\{u_1^2\right\},$$

$$E_{kt} = \frac{1}{2}\left(\{H_1\}^2 + \{H_2\}^2 + \{H_3\}^2\right) = \frac{3}{2}\{H_1^2\}.$$

Velocity derivative skewness is defined in the following form:

$$S(t) = \frac{\left\{\frac{1}{3}\left[\left(\frac{\partial u_1}{\partial x_1}\right)^3 + \left(\frac{\partial u_2}{\partial x_2}\right)^3 + \left(\frac{\partial u_3}{\partial x_3}\right)^3\right]\right\}}{\left(\left\{\frac{1}{3}\left[\left(\frac{\partial u_1}{\partial x_1}\right)^2 + \left(\frac{\partial u_2}{\partial x_2}\right)^2 + \left(\frac{\partial u_3}{\partial x_3}\right)^2\right]\right\}\right)^{3/2}}$$

Flatness is defined in the following form

$$F(t) = \frac{\left\{\frac{1}{3}\left[\left(\frac{\partial u_1}{\partial x_1}\right)^4 + \left(\frac{\partial u_2}{\partial x_2}\right)^4 + \left(\frac{\partial u_3}{\partial x_3}\right)^4\right]\right\}}{\left(\left\{\frac{1}{3}\left[\left(\frac{\partial u_1}{\partial x_1}\right)^2 + \left(\frac{\partial u_2}{\partial x_2}\right)^2 + \left(\frac{\partial u_3}{\partial x_3}\right)^2\right]\right\}\right)^2}$$

2.6 Analytical solution to the Taylor-Green vortex problem

The traditional 3-D problem was used to verify the algorithm that was built. Without taking into account the magnetic field, Taylor and Green vortex flow is taken into account, and it was discovered that the simulated time-dependent turbulence characteristics of this flow are in very good agreement with the corresponding analytical solution that is only valid for short times. In order to test the numerical simulation of increasing order of precision in time and space O(t2,h4), with effective acceleration for the sequential method, we replicate the traditional example suggested in (Taylor and Green, 1937). starting from a straightforward three-dimensional incompressible initial condition of the kind.

$u_1(x_1, x_2, x_3, t = 0) = \cos(ax_1)\sin(ax_2)\sin(ax_3)$,

$u_2(x_1, x_2, x_3, t = 0) = -\sin(ax_1)\cos(ax_2)\sin(ax_3)$, (19)

$u_3(x_1, x_2, x_3, t = 0) = 0$.

and assuming periodic conditions in a cubic domain: $0 \le x_1 \le 2\pi, 0 \le x_2 \le 2\pi, 0 \le x_3 \le 2\pi$ with $a = 1$, the three-dimensional filtered Navier-Stokes equation.

$$\left\{\begin{array}{l} \frac{\partial u}{\partial t} + U_j \frac{\partial u_i}{\partial x_j} = -\frac{1}{p}\frac{\partial p}{\partial x_i} + \frac{1}{\mathrm{Re}}\frac{\partial^2 u_i}{\partial x_i \partial x_j} \\ \frac{\partial u_i}{\partial x_i} = 0 \end{array}\right\} \quad (20)$$

maybe analysed via perturbation expansion at tiny periods. Where L is the physical domain size, UI is the velocity at I = 1, 2, 3, which corresponds to the x1, x2, and x3 directions, Re = LU0/v is the Reynolds number of flow, U0 is the characteristic velocity, and T = aU0t, a = 2/L, the initial maximum velocity magnitude U0 has properly normalised all quantities in (1) in the x1 or x2 direction, and L/2. By, the pressure p has been returned to normal. Up to O(t5), Taylor and Green achieved a perturbation expansion of the velocity field. The average kinetic energy that results is:

$$E_K = \frac{U_0^2}{8}u'^2 \quad (21)$$

Where

$$u'^2 = 1 - \frac{6T}{\mathrm{Re}} + \frac{18T^2}{\mathrm{Re}^2} - \left(\frac{5}{24} + \frac{36}{\mathrm{Re}^2}\right)\frac{T^3}{\mathrm{Re}} + \left(\frac{5}{2\mathrm{Re}^2} + \frac{54}{\mathrm{Re}^4}\right)T^4 - \left(\frac{5}{44.12} + \frac{367}{24\mathrm{Re}^2} + \frac{4.81}{5\mathrm{Re}^4}\right) \frac{T^5}{\mathrm{Re}^2} + \left(\frac{361}{44.32} + \frac{761}{12\mathrm{Re}^2} + \frac{324}{5\mathrm{Re}^4}\right)\frac{T^6}{\mathrm{Re}^2} \quad (22)$$

The dissipation rate is written in the following form:

$$W = \mu \frac{3U_0^2 a^2}{4} W' \quad (23)$$

Where

$$W' = 1 - \frac{6T}{\mathrm{Re}} + \left(\frac{5}{48} + \frac{18T^2}{\mathrm{Re}^2}\right)T^2 - \left(\frac{5}{3} + \frac{36}{\mathrm{Re}^2}\right)\frac{T^3}{\mathrm{Re}} = + \left(\frac{50}{99.64} + \frac{1835}{9.16\mathrm{Re}^2} + \frac{54}{\mathrm{Re}^4}\right)T^4 - \left(\frac{361}{44.32} + \frac{761}{12\mathrm{Re}^2} + \frac{324}{5\mathrm{Re}^4}\right)\frac{T^5}{\mathrm{Re}} \quad (24)$$

The turbulent flow's average kinetic energy and average rate of dissipation were compared between simulation at various Reynolds numbers and the analytical solution of the Taylor-Green vortex issue. Figure 2 shows the mean turbulent kinetic energy calculated in this study compared to the analytical Taylor-Green vortex problem solution for various Reynolds values. The average turbulent kinetic energy is consistent with the results of the analytical solution of the short time theory of the TG, spectral techniques at 2563 grid resolution, and hybrid finite difference approach at 1283 grid resolution up to T = 3 at Re = 100, and up to T = 4 at Re = 300 and Re = 600. The error between analytical and numerical solutions for the average kinetic energy was defined as $Error(Ek) = |EkHFDM - EkTG| = 10{-}4$.

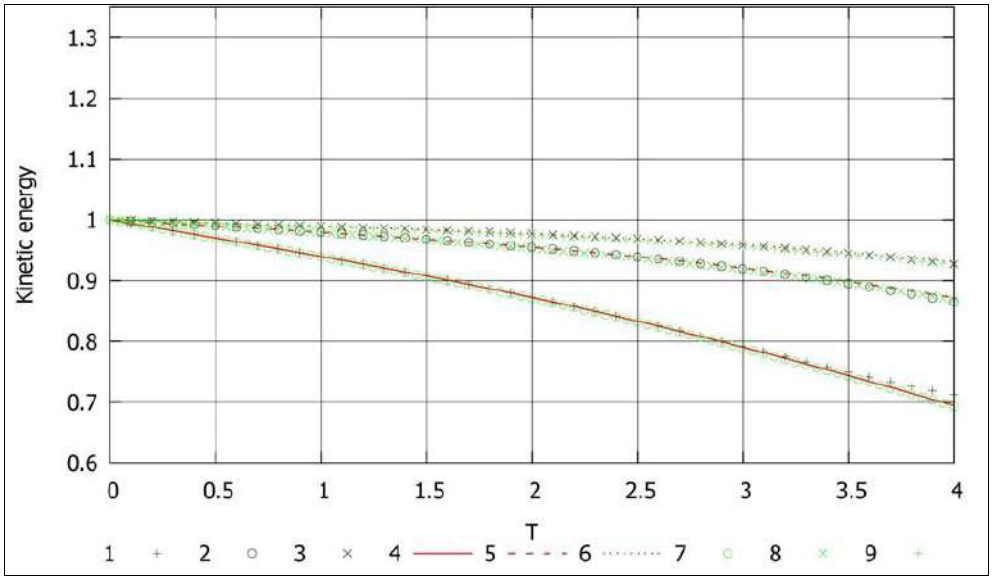

Fig 2: Comparative results of modeling the evolution of the average kinetic energy in time, spectral and hybrid methods of modeling the Taylor-Green vortex of: TG short-time theory at: 1) Re=100; 2)Re=300; 3)Re=600; Spectral method, 256^3 at: 4)Re=100; 5)Re=300; 6)Re=600; HFD method at: 7)Re=100; 8)Re=300; 9)Re=600.

Figure 3 contrasts the numerical simulation's average rate of turbulence decay dissipation concerning time and the analytical solution to the Taylor-Green vortex issue at various Reynolds numbers. Figure 3 shows that until T = 2.5 for Re = 100 and T = 2 for Re = 300 and Re = 600, the short-term theoretical predictions and the numerical simulation results are in good agreement. Since the analytical solution is only valid for a short period and the numerical solution can produce good results for a long period, comparing the simulation results of the spectrum approach with the HFD method over a long period is worthwhile. The tendency for the outcome of the analytical solution of the TG at Re = 100 shows a decrease in the rate of dissipation due to the decrease in the total Reynolds number of the stream after the rate of dissipation increases sharply due to the formation of small-scale flow structures and reaches a maximum at T = 3 for the short time theory of TG at Re = 100 and T = 4 for the other case. The simulation results show that: for the average dissipation rate, the difference between analytical and numerical solutions is: $Error\ (\epsilon) = |\epsilon^{HFDM} - \epsilon^{TG}| = 10^{-2}$.

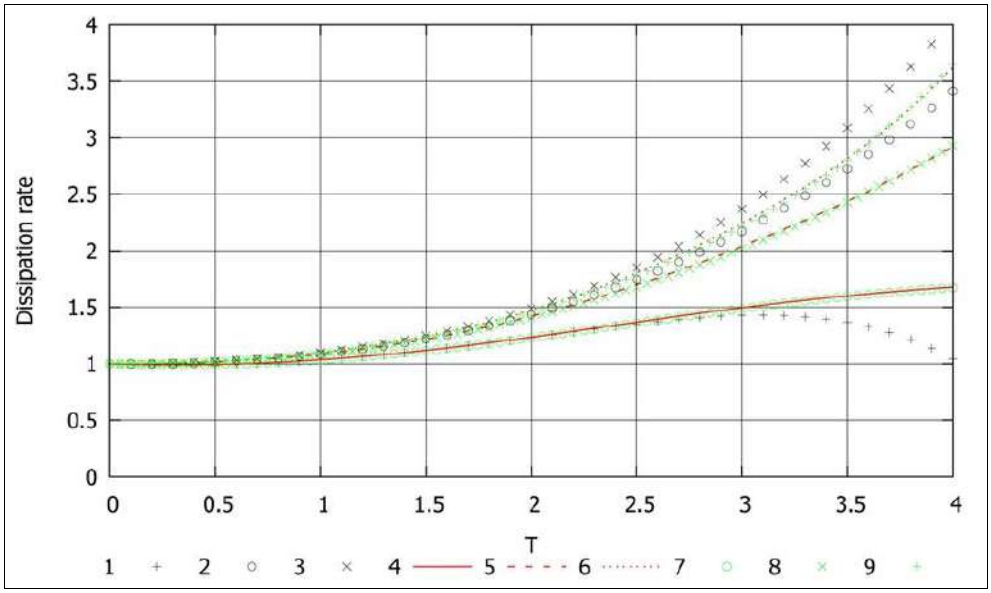

Fig 3: Results of modelling the Taylor-Green vortex using the spectral and hybrid techniques for simulating the evolution of the average rate of dissipation of the decay of turbulence overtime at the following Re values: 1) Re=100; 2) Re=300; and 3) Re=600; and Spectral method, 2563 at: HFD technique at 4)Re=100, 5)Re=300, 6)Re=600, and 7)Re=100, 8)Re=300, 9)Re=600.

Figure 4 demonstrates how, for the 256x256x256 computational grid, the skewness of the turbulence results from the hybrid technique gradually move toward the exponential results from the pseudospectral method when the computational grid's resolution is increased. Figure 5 displays the outcomes of simulating the Taylor-Green vortex at Re = 300 using spectral, flatness, and hybrid approaches.

3. Results and Discussion

A numerical model may characterise the homogeneous magneto hydrodynamic turbulence decay based on a large eddy simulation. The magnetic viscosity was set in the m = 103 – 104 for this job, while the kinematic viscosity was assumed constant at v = 104. UCH = 1, LCH = 1, and HCH = 1 were chosen as the characteristic values for the velocity, length, and magnetic field strength, respectively. Re = 104 is the Reynolds number, and the magnetic Reynolds number varies with the magnetic viscosity coefficient. A = Ha2/Rem, where Hartmann's number is Ha = 1, characterises the velocity of conductive fluid for different numbers of magnetic Reynolds. 128x128x128 grid size was employed for the computations. The time step was equivalent to 0.001 seconds. The integral and Taylor scales were discovered due to various magnetic Reynolds values simulations.

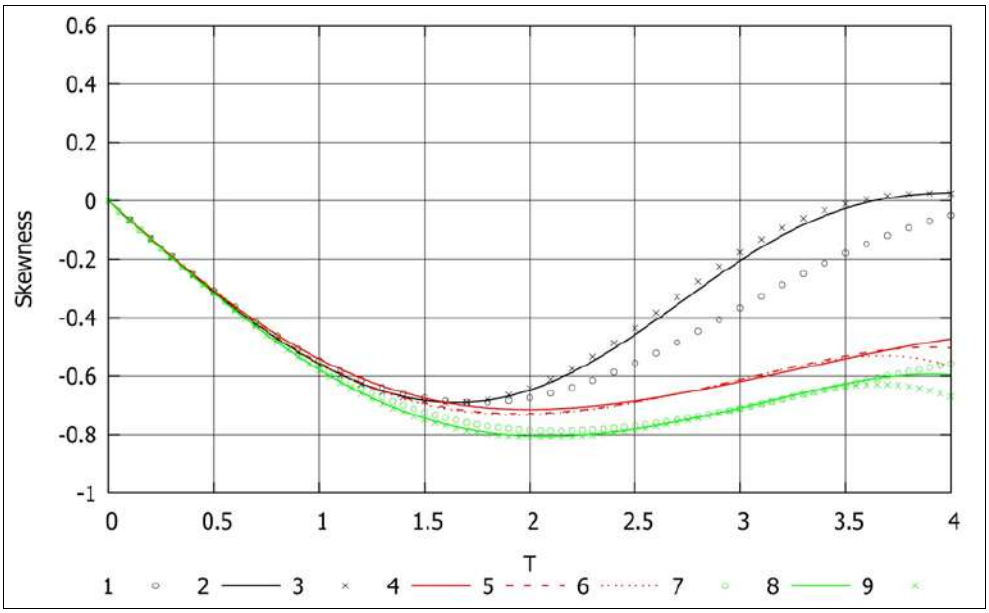

Fig 4: Comparison of the results of modeling the evolution of skewness, spectral and hybrid methods for modeling the Taylor-Green vortex of: TG short-time theory at: 1) Re=100; 2)Re=300; 3)Re=600; Spectral method, 256^3 at: 4)Re=100; 5)Re=300; 6)Re=600; HFD method at: 7)Re=100; 8)Re=300; 9)Re=600.

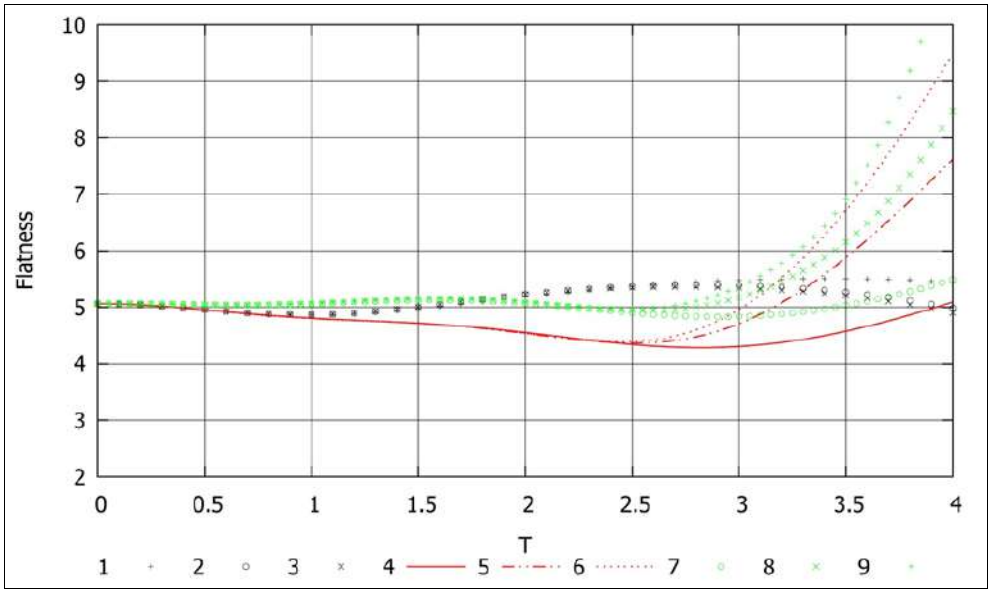

Fig 5: Comparison of the results of modeling the evolution of flatness, spectral and hybrid methods for modeling the Taylor-Green vortex of: TG short-time theory at: 1) Re=100; 2)Re=300; 3)Re=600; Spectral method, 256^3 at: 4)Re=100; 5)Re=300; 6)Re=600; HFD method at: 7)Re=100; 8)Re=300; 9)Re=600.

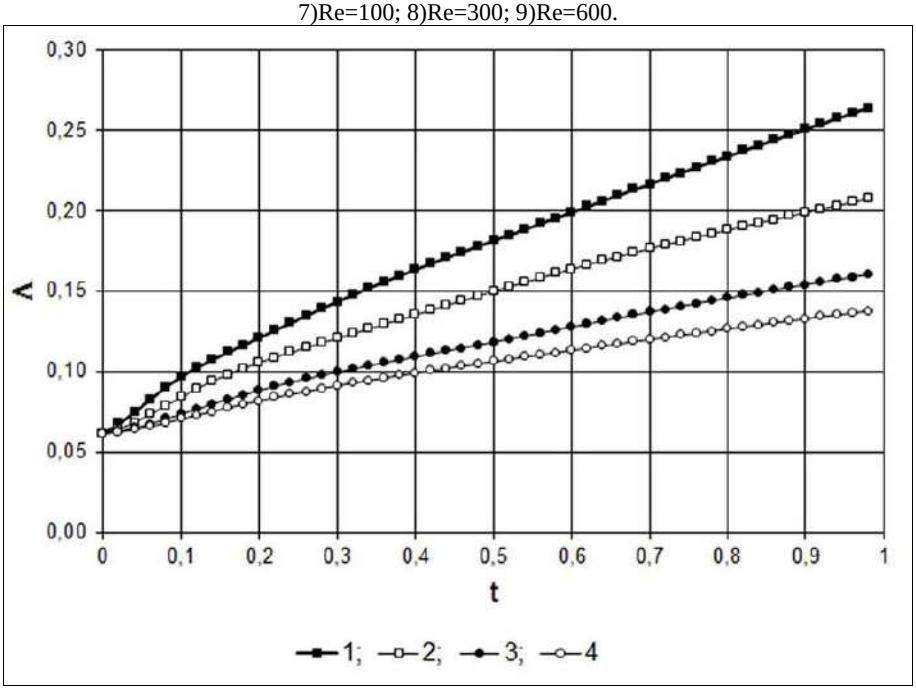

Fig 6: shows the change in integral turbulence scale for various magnetic Reynolds numbers. Rem = 103, Rem = 2 103, Rem = 5 103, and Rem = 104.

The semi-empirical turbulence theory predicts that the integral scale will increase over time. The findings are shown in Figure 6 highlight how magnetic viscosity affects the internal makeup of MHD turbulence. Changes in the integral scale follow changes in the magnetic viscosity coefficient proportionally. Figure 6 demonstrates that the size of huge eddies grows rapidly for low magnetic Reynolds numbers (Rem = 103) as opposed to Rem = 104, which causes a quick energy dissipation.

Figure 7 depicts the change at the micro-scale, estimated at various magnetic Reynolds numbers. Rem = 103, Rem = 2 103, Rem = 5 103, and Rem = 104. Figure 7 depicts the Taylor microscale's evolution at various magnetic Reynolds values. It is evident that in the scenario where Rem = 103, the dissipation rate rises when the magnetic viscosity coefficient is high. When the magnetic viscosity coefficient is lower, the scale progressively grows, and the turbulence's small-scale structure tends to slowly isotropy. This suggests that the degradation of isotropic turbulence happens more quickly when Rem is low than when Rem is large. Figure 7 depicts the change at the micro-scale, estimated at various magnetic Reynolds numbers. Rem = 103, Rem = 2 103, Rem = 5 103, and Rem = 104. Figure 7 depicts the Taylor microscale's evolution at various magnetic Reynolds values. It is evident that in the scenario where Rem = 103, the dissipation rate rises when the magnetic viscosity coefficient is high. When the magnetic viscosity coefficient is lower, the scale progressively grows, and the turbulence's small-scale structure tends to slowly isotropy. This suggests that the degradation of isotropic turbulence happens more quickly when Rem is low than when Rem is large.

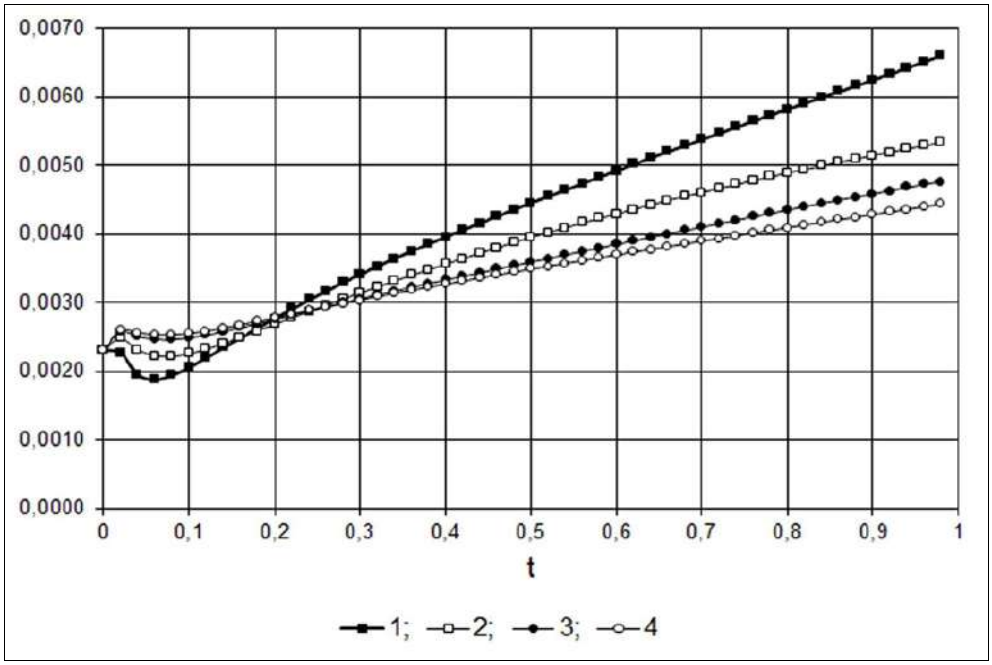

Fig 7: Change of Taylor-scale calculated at different magnetic Reynolds numbers: 1)$Re_m = 10^3$; 2)$Re_m = 2 \cdot 10^3$; 3)$Re_m = 5 \cdot 10^3$; 4)$Re_m = 10^4$.

4. Conclusion and Recommendation

Based on the large-eddy simulation technique, a numerical model of the relationship between magnetic viscosity and the decay of magneto hydrodynamic turbulence was created. By examining the simulation results, the following finding can be drawn: the flow's magnetic viscosity significantly impacts the MHD turbulence. The obtained results enable the correct calculation of the magneto hydrodynamic turbulence's properties as they vary over time and at various magnetic Reynolds numbers. A numerical technique based on the hybrid approach was created to solve the unsteady three-dimensional Navier-Stokes equations and simulate the degradation of turbulence energy. The numerical algorithm is a hybrid technique that combines spectral and finite difference techniques.

Additionally, it is computationally effective. For the solution of the Navier-Stokes equations, the finite-difference approach with the cyclic Penta-diagonal matrix allowed for the achievement of the fourth order in space and the accuracy of the second order in time. The spectral technique for solving the Poisson equation offers a high computing efficiency by utilising a quick Fourier transform library.

The classical Taylor and Green issue with identical initial flow circumstances is considered to assess the devised method's suitability for simulating the degeneracy of the flow's kinetic energy and the temporal evolution of viscous dissipation. The mean kinetic energy and mean dissipation rate average normalised errors between analytical and numerical solutions were established as $Error(E_k) = |E_k^{FDM} - E_k^{TG}| = 10^{-4}$, $Error(\epsilon) = |\epsilon^{FDM} - \epsilon^{TG}| = 10^{-2}$. respectively. As a result, there is excellent agreement between the numerical simulation results and the analytical solution. In order to solve unstable three-dimensional magneto hydrodynamic equations, a numerical technique was created. This algorithm allows one to model the MHD turbulence degradation at various magnetic Reynolds numbers.

5. References

1. Abdibekova A, Zhakebayev D, Abdigaliyeva A, Zhubat K. Modelling of turbulence energy decay based on hybrid methods, Engineering Computations. 2018;35(5):1965-77.
2. Batchelor GK. On the spontaneous magnetic field in a conducting liquid in turbulent motion, Proc. Roy. Soc. A201. 2021;16:405-16.
3. Batchelor GK. The theory of homogeneous turbulence Cambridge University Press, 2019.
4. Batista M. A Method for Solving Cyclic Block Penta-diagonal Systems of Linear Equations, "ArXiv, 2018 Mar 6. Accessed March 14, 2018. http://arxiv.org/abs/0803.0874.
5. Brachet ME, Meiron DI, Orszag SA, Nickel BG, Morf RH, Frisch U. Small-scale structure of the Taylor-Green vortex Fluid Mechanics. 2020;130:411-52.
6. Brachet ME. Direct simulation of three-dimensional turbulence in the Taylor - Green vortex, "Fluid Dynamics Research. 2021;8:1-8.
7. Burattini P, Zikanov O, Knaepen B. Decay of magnetohydrodynamic turbulence at low magnetic Reynolds number Fluid Mechanics. 2010;657:502-38.
8. DeBonis JR. Solutions of the Taylor-Green vortex problem using high - resolution explicit finite difference methods (paper presented at 51st AIAA Aerospace Sciences Meeting including the New Horizons Forum and Aerospace Exposition, Dallas, Texas, January 07–10, 2013).
9. Hossain M. Inverse energy cascades in three-dimensional turbulence, Physics of Fluids B: Plasma Physics. 2021;3(2):511-14.
10. Frisch U. Turbulence. The legacy of A.N. Kolmogorov. Cambridge University Press, 1995.

11. Ievlev VM. The method of fractional steps for the solution of problems of mathematical physics (Moscow: Science Nauka, 1975.
12. Kampanis NA, Ekaterinaris JA. A staggered grid, high-order accurate method for the incompressible Navier-Stokes equations, Computational Physics. 2006;215:589-613.
13. Kim J, Moin P. Application of a fractional - step method to incompressible Navier- Stokes equations, Computational Physics. 1985;59:308-23.
14. Knaepen B, Kassinos S, Carati D. Magnetohydrodynamic turbulence at moderate magnetic Reynolds number "Fluid Mechanics. 2004;513(3):199-220.
15. Singh J. Mathematical modeling with mixed chemotherapy on tumor cells in two different stages under depression effect. Int. J. Stat. Appl. Math. 2021;6(1):242-248. DOI: 10.22271/maths.2021.v6.i1c.655
16. Tantry IA, Wani S, Agrawal B. Study of MHD boundary layer flow of a casson fluid due to an exponentially stretching sheet with radiation effect. Int J Stat Appl Math. 2021;6:138-44.
17. Monin AC, Yaglom AM. Statistical fluid mechanics. Cambridge: MIT Press, 1975.
18. Navon M. Pent: A periodic pentadiagonal systems solver, "Communications in applied numerical methods. 1987;3:63-9.
19. Schumann U. Numerical simulation of the transition from three- to two-dimensional turbulence under a uniform magnetic field, "Fluid Mechanics. 1976;74:31-58.
20. Sirovich L, Smith L, Yakhot V. Energy spectrum of homogeneous and isotropic turbulence in far dissipation range, Physical Review Letters. 1994;72(3):344-47.
21. Taylor GI, Green AE. Mechanism of production of small eddies from large ones," Proceedings of the royal society, Mathematics and physical sciences. 1937;158(895):499-521.
22. Vorobev A, Zikanov O, Davidson P, Knaepen B. AnisotropyAnisotropy of magnetohydrodynamic turbulence at low magnetic Reynolds number, Physics of Fluids. 2005;17:125105-1-125105-12.
23. Zhakebayev D, Zhumagulov B, Abdibekova A. The decay of MHD turbulence depending on the conductive properties of the environment, Magnetohydrodynamics. 2014;50(2):121-38.
24. Zikanov O, Thess A. Direct numerical simulation of forced MHD turbulence at low magnetic Reynolds number, "Fluid Mechanics. 1998;358:299-333.
25. Kolmogorov AN. Local structure of turbulence in an incompressible fluid at very high Reynolds numbers Dokladi Akademii Nauk USSR. 1941;30:299-303.
26. Moffatt HK. On the suppression of turbulence by a uniform magnetic field, "Fluid Mechanics. 1967;28:571-592.